



Particle Physics and Astronomy
Research Council

Royal Greenwich Observatory

wht-naomi-77

AOW/WFS/ABG/5.1/5/97 2ccdpr.doc

NAOMI Adaptive Optical System Project Report

2 CCD WFS architecture - PDR document

B Gentles, AWeise, S Worswick

Issue 1.0; 22 May 1997

**Royal Greenwich Observatory,
Madingley Road,
Cambridge CB3 0EZ**

Telephone (01223) 374000
Fax (01223) 374700
Internet ngs@ast.cam.ac.uk

1. INTRODUCTION	4
2. THE CONCEPT	4
3. WHAT THE WFS CAMERA IS REQUIRED TO DO.	4
3.1. WFS camera functional and performance requirements	4
3.2. Modes of operation	6
3.3. 4x4 baseline pixel mode description	6
3.4. other options	7
4. DERIVED REQUIREMENTS	7
4.1. Latency, noise and architecture	7
4.2. Alignment and Stability	11
4.3. laser upgrade	12
4.4. ghosting	12
4.5. Alignment Error Budget - general.	13
4.6. positioning	14
4.7. data processing	14
5. HARDWARE PROPOSAL	14
5.1. System geometry	15
5.2. Figure 5-2 Orientation of focal planes in the WFS	15
5.3. Optical Layout	16
6. DETAILED DESCRIPTION	16
6.1. Optics	16
6.2. Mechanical Assembly	19
6.3. Alignment and integration	25
6.4. CCD Controller and software	25
6.5. Frame data packets.	28
6.6. Detector	28
7. INTERFACES	29
7.1. Optical	29

7.2. Mechanical	29
7.3. Electrical	29
7.4. Software	30
8. COST AND PROCUREMENT ISSUES.	30
APPENDIX 1. DOCUMENT HISTORY	32
APPENDIX 2. CCD DATA PACKET PROTOCOL.	33
Introduction	33
Physical Layer	33
Serial data word packet format	33
Parallel data word format.	33
Data codes	33
Frame packet structure	35
APPENDIX 3. SIMPLE TEST TO PROVE ALIGNMENT OPERATIONS	37
XY Positioning of CCD Head	37
Repeatability of BS Slide	37
APPENDIX 4. SDSU READOUT TIME ESTIMATES	39
APPENDIX 5. SKY COVERAGE ISSUES FOR AN INCREASED NOISE SENSOR.	40
APPENDIX 6. 4X4 BASELINE MODE JUSTIFICATION	41
APPENDIX 7. 1D AND 2D CENTROIDS	42
APPENDIX 8. GEMINI ICD 1.6.1/1.6.2 - A&G TO WFS SYSTEM.	43

1. Introduction

This document proposes a new architecture for the NAOMI WFS camera. It includes the background detail to justify this choice. The document is structured as follows:

Section 2 summarises the concept of the change and the generic reasons for choosing it.

Section 3 describes those functional and performance criteria which this subassembly of the WFS has to meet.

Section 4 derives the generic requirements on a camera system, proposes and justifies the proposed architecture.

Section 5 summarises the actual hardware proposed.

Section 6 describes the proposed system in depth.

2. The Concept

At the WFS PDR in February 1997, a preliminary design of the NAOMI WFS was presented. It had a conventional optical layout containing a camera which imaged a lenslet array on a single small CCD. At that time, the diverse requirements of low noise at low frame rate and very low latency at high frame rate could not be met by any one known current CCD controller. Existing fast CCD controllers did not give any gain in signal to noise at low frame rates and those cameras which could give good noise at low frame rates could not operate fast enough to meet the clause A requirement.

It occurred to us that the basic post processing consists of measuring X and Y centroids of the spots in each subaperture. This is usually done by taking marginal sums in X and Y and then using the 1D images to estimate the image centroid in each direction. If we could avoid the need to readout the 2D image then we could read less pixels; thus we could spend more time on each one for the same readout latency. This was the aim of this architecture.

The WFS design proposed here moves the point in the processing chain where the XY separation is done from in a computer to inside the CCD. The marginal sums are calculated by collecting charge in the readout register of the CCD, thus only reading out a 1D image from the chip. Separate CCD's are used for X and Y so that the efficiency of vertical binning on the CCD is utilised. We gain in two ways:

?? The light is collected before readout, so we only get the readout noise once per marginal sum sample rather than in every pixel. => less noise

?? We read less pixels so each one can take more time with less noise. => less noise or lower latency

?? Slower max pixel rate means that a single existing controller will meet all our requirements.

?? We need not develop any new controller hardware. => less technical risk

The method is not without its disadvantages though:

?? The light has to be split between 2 CCD's so each gets less signal.

?? The controller is more complex.

3. What the WFS camera is required to do.

3.1. WFS camera functional and performance requirements

Name	value	units	WPD ref	Section	Description
Basic function					Image spots onto CCD detector
4x4 pixel mode					centroid spots with 4x4 box

quadCell mode					centroid spots with quadcell box
spot raster distortion	0.2	pix			Limit of movement of any spot from subaperture centre due to WFS fixed aberrations. Applies to quad cell mode only.
readout noise - max rate	7 0.0031	erms pix (10k phot)			ccd read noise at max rate. rms centroid error derived from 4x4 centroid propagator with 10k photons. Section 4.1. goal is 5 erms. = 0.0022 pix rms.
readout noise - 100 kPix/s	3 0.067	erm pix (200 phot)			ccd read noise at 100 kpix/s, rms centroid error derived from 4x4 centroid propagator with 200 photons. Section 4.1. goal is 2 erms.= 0.045 pix rms
flexible readout scheme					To allow other readout modes to be developed & used.
on the fly change of readout mode					change of readout mode without interrupting frame rate.
Latency	300	? s			Max frame readout and centroiding time. From end of integration to last centroid calculated in RTCS. 8x8 subset of 10x10 subapertures. Applies only to 4x4 baseline at max rate. Relaxation of spec in WPD by agreement with PS & PE.
Read noise varies with pixel rate.					To provide operational flexibility to allow for lower read noise when operating with faint stars.
space envelope					To fit in WFS space envelope.
Max frame rate	1	kHz			For good servo performance with bright stars.
Pixel digitisation	12	bits			Min number of pixels to digitise CCD data to.
CCD	4	port			Must use a high efficiency 4-port Frame transfer CCD.
Laser beacon upgrade					We must be able to operate as a tracker for the planned laser upgrade.

--	--	--	--	--	--

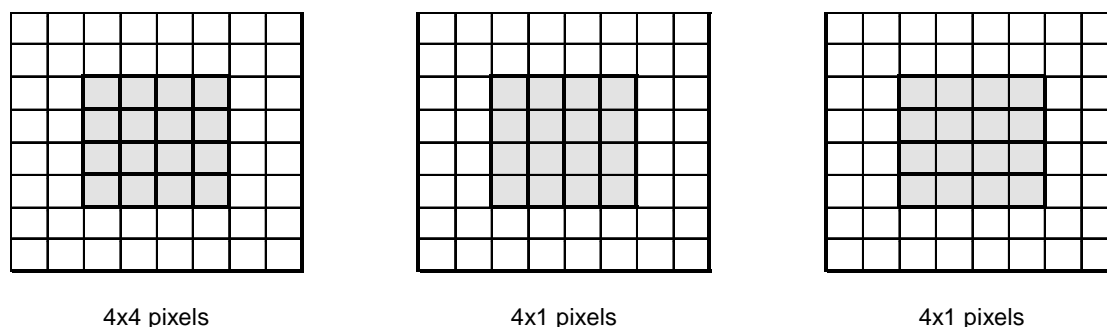
3.2. Modes of operation

4x4 pixel centroid	<p>Baseline mode. Used when the spot excursions are likely to be large, ie bad seeing or large non zero servo-loop working points.</p> <p>Linear relation with spot error and centroid.</p> <p>Noise is worse than 4x4</p> <p>Latency is worse than 4x4</p> <p>The 0.2 pixel spot position spec does not apply.</p>
Quad-cell mode	<p>Used in cases of small spot excursions: good seeing and on-axis work.</p> <p>Best noise performance Best latency.</p> <p>Spot working point must be within the linear region of the transfer curve. Depends on spot profile.</p>
6x6 pixel	used in bad seeing with wider spots or larger excursions, or to acquire in bad seeing.
8x8 pixel	used for open loop measurements and for acquisition in bad seeing.

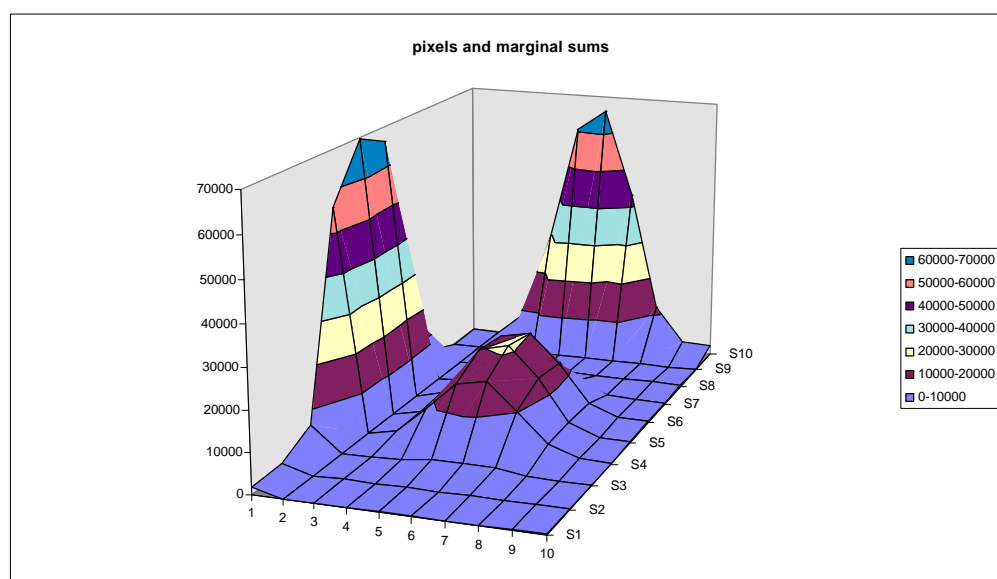
3.3. 4x4 baseline pixel mode description

The baseline ccd readout scheme, which is shown in Figure 3-1, uses 8x8 CCD pixels for each subaperture. The WFS optics are required to image a spot on the centre of the 8x8 box to within 0.2 pixels. The centre 4x4 box, shown shaded grey, is read out providing 16 pixels with a guard band of 4 pixels before the next active pixel is encountered. The diffraction limit of the subaperture is 1.8 pixels across, at 0.51 arcsecs.

Figure 3-1 Baseline subaperture readout geometry

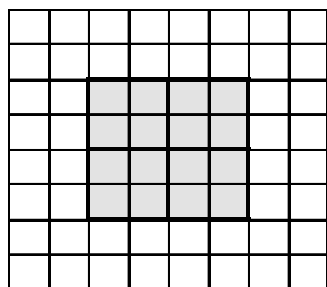


To illustrate the processing required, consider the star shown in Figure 3-2. The 3D graphic shows the star profile in the centre and the marginal sums of rows and columns can be seen on each side of the cube. If the marginal sums were done on chip then there is clearly better signal to noise.

Figure 3-2 3D star profile and marginal sums

3.4. Other options

The quad cell mode is required for use with objects close to the guide star where the systematic aberrations are small and the working position for each spot is close to the centre of the sub-aperture. If the spots are within 0.5 pixels of the centre line, the 4 pixels can be binned into 4 large pixels forming a quad cell about the subaperture centre. This is shown in Figure 3-3.

Figure 3-3 Quad-cell readout geometry

This geometry means that only 4 pixels are sampled in each subaperture. This should allow the fastest readout times and lowest latency. Note that the transfer function of spot position to measured position is non linear, and falls off rapidly either side of the central region. This is why the quad cell can only be used with spots near to the origin.

4. Derived Requirements

4.1. Latency, noise and architecture

We have modelled the readout of a 4 ports CCD39 chip for various controller parameters, including pixel sampling time, charge transfer time, pipelining and data transfer bottlenecks

From the CCD readout model, we have a range of readout schemes which allow us to relate the CCD read noise to the frame readout latency. The noise propagation through the standard centroid algorithm has been modelled and the following relation derived.

$$Error_{centroid} = \frac{noise^2 \cdot N_y \cdot \frac{N_x}{x^2} \cdot \frac{N_x}{2} \cdot 0.5 \cdot N_b^2}{P^2 \cdot N_x \cdot N_y \cdot noise^2}$$

where *noise* is the CCD readout noise in electrons rms,
 N_x is the number of samples in the X direction,
 N_y is the number of samples in the Y direction,
 N_b is the number of samples binned in the X direction,
 P is the number of detected photons in the subaperture.

For the 4x4, 6x6 and 8x8 cases, $N_b = 1$. For the Quad-cell, $N_b = 2$ to account for the larger pixel sizes.

Figure 4-1 CCD39 noise vs speed graph

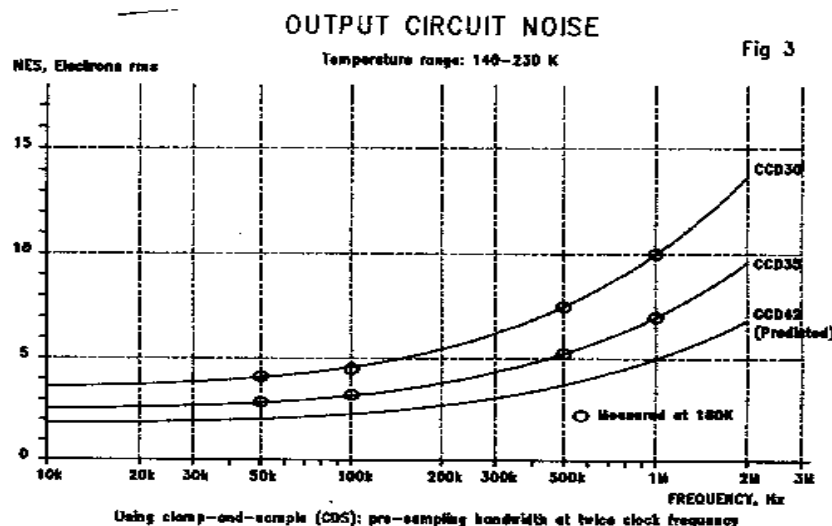
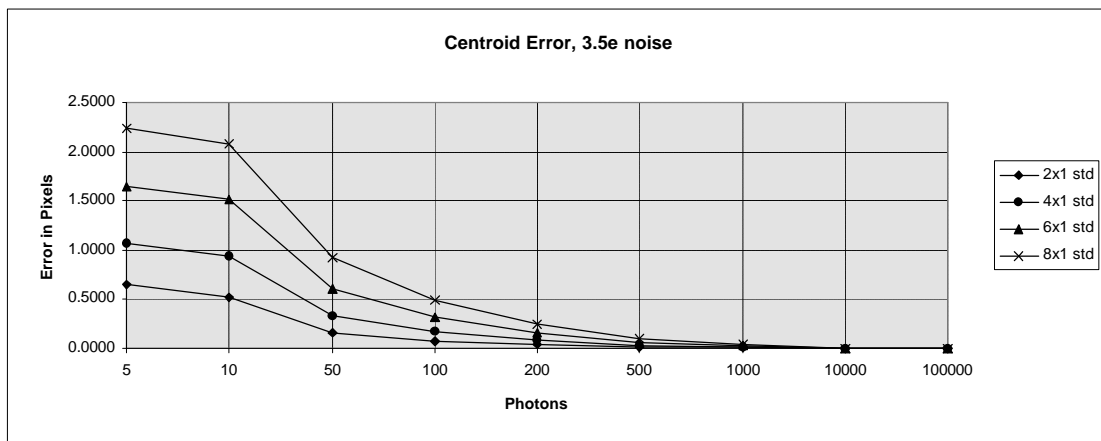


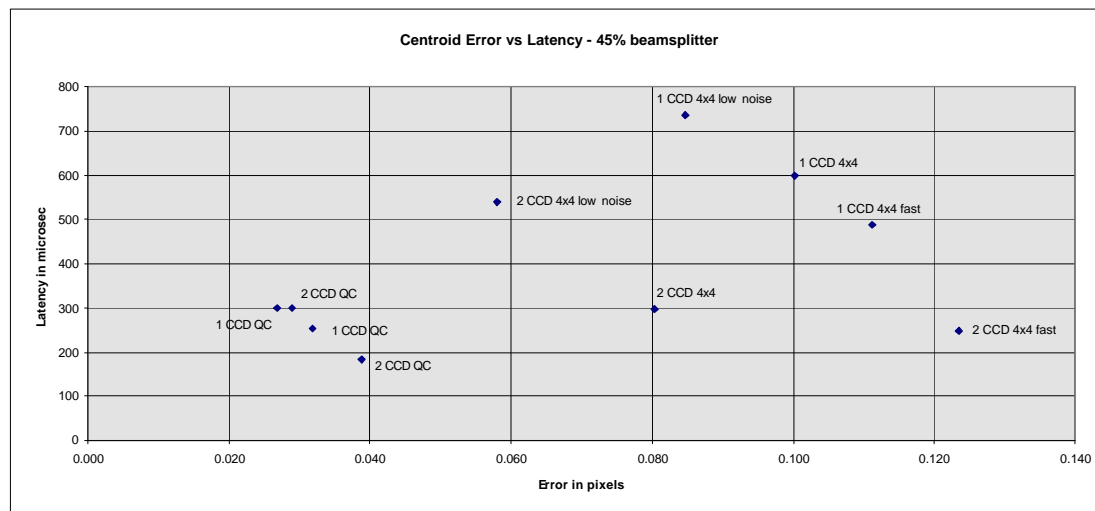
Figure 4-2 shows the results for Quad-cell, 4x4, 6x6 and 8x8 modes. All are read out in the 2-CCD case with 4 pixel vertical binning and no horizontal binning. $N_x = 2, 4, 6, 8$; $N_y = 2, 4, 6, 8$; $N_b = 1$. A SDSU controller reading at a “standard” rate was assumed. We have used $P = 200$ detected photons to model a demanding case with a faint star.

Figure 4-2 Centroid Error due to binning



The model was used to derive a relationship between pixel error and latency for both the Quad-cell mode and the 4x4 baseline mode. This allows us to derive a common figure of merit for the various modes. Figure 4-3. shows the relation between centroid error and operating mode.

Figure 4-3 noise comparison.

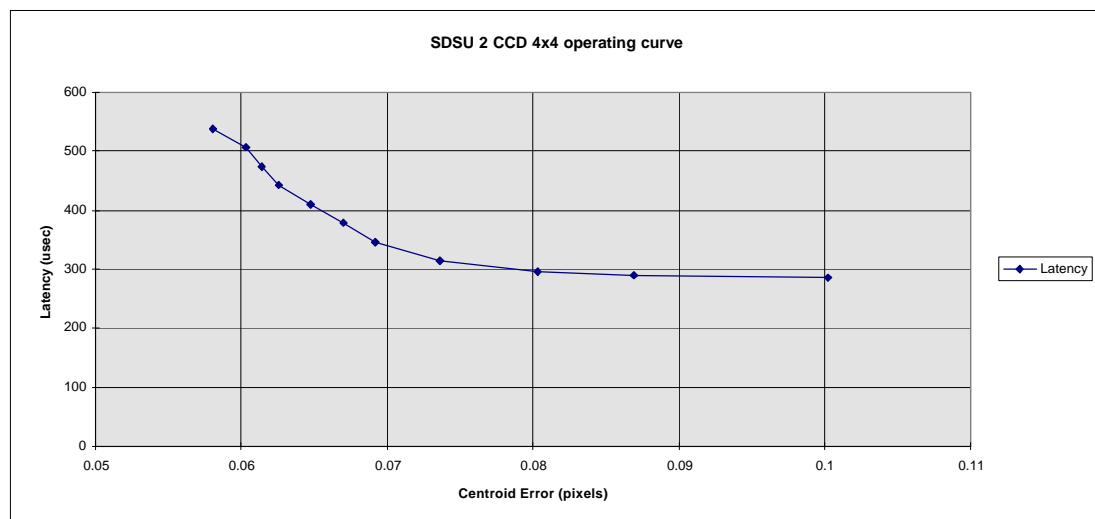


The required latency of 300 μ s is achieved by all Quad cell modes and some of the 2CCD modes.

Separate analysis has shown that the centroiding can be performed in parallel with the frame readout, with a pipeline overhead of approximately 2.5 μ sec. In comparison to the frame time, this is negligible and will be ignored here.

The 4x4 timings shown above assume a slight improvement on the CCD39 readout waveforms used in the Gemini PWFS. The fast mode plotted above is within the capability of the camera but has not yet been proven with the CCD39. We can derive an operating curve for the camera system by calculating centroid error for a series of pixel times and plotting the resulting latency vs centroid error. This is shown in Figure 4-4 below.

Figure 4-4 4x4 with 2 CCD operating curve



The baseline requirement has two aspects to it, high speed, low latency operation and low speed, low noise operation with the noise related to frame rate. for single CCD detector, these lead to completely different CCD readout regimes and differing CCD hardware. We do not know of a commercially

available controller which will provide both these readout regimes. If we choose the 2CCD route, the required pixel rates drop from the order of 2 Mpix/sec to approx 400 kPix per second for the 4x4 baseline mode. This brings the pixel rate down to that achievable by a standard commercially available controller.

Routes to solve this problem by utilising two separate controllers are possible but have been discarded on grounds of complexity and cost.

A 2CCD architecture with conventional slow-scan CCD controller is thus proposed on both noise, latency and availability grounds. For the 4x4 baseline mode, this wins on all performance counts. It is more complex, with 8 ports and 2 heads, but still a standard part.

When operating in Quad-cell mode, the 2-CCD architecture suffers a 3.4 % loss in sky coverage [see Appendix D]. Two routes are possible to solve this, either by slowing down the pixel rate to drop the read-noise or to physically remove the beamsplitter allowing more light to reach a single detector. Operating in Quad-cell mode with a conventional controller, the latencies for both 1-ccd and 2-ccd operation are acceptable.

Discussion with the Project scientist has established that he would prefer to implement an extra mechanism rather than sacrifice sky-coverage. We thus propose to implement a mechanism to remove the beamsplitter from the path when required. The beamsplitter slide would swap the glass beamsplitter for a plain glass element to keep the optical path length constant. Non repeatability of the beamsplitter would cause movement of the image down one of the paths which would appear as a tilt error and be removed during acquisition. Thus there is no tight requirement for beamsplitter position repeatability.

We propose to operate with the 1-CCD configuration in quad-cell mode and with the 2-CCD configuration in all other modes.

We propose not to move the beamsplitter during an observation.

In the unlikely event of conditions being bad enough to require acquisition in 4x4 mode, then improving such that switching from 4x4 to quad-cell mode is desired, this could be allowed with the AO loop locked, by remaining in 2-CCD mode and accepting the slight loss in read-noise performance for the much larger gain by moving to Quad-cell. The Beamsplitter will not be moved in this scenario.

4.2. Alignment and Stability

The alignment procedure and error analysis are essentially the same for the WFS with 1 or 2 CCD's.

The aberration specification of 0.2 pixels for all spots provides an upper bound on the spot movements caused by the following causes:

- ?? Misalignments
- ?? Optical manufacturing errors
- ?? Stability of optical components with time and temperature.
- ?? repeatability of slides.

This requirement is unchanged from the WFS PDR design.

The beamsplitter is an extra component which has been included in the figuring allocation of the distortion error budget. It does not materially affect the straight through path other than transmission and ghosting.

The beam splitter position and tilt alignment and repeatability affect the image on the Second CCD directly. The sensitivity to tilt errors is strong, 0.004 degrees will cause a 0.1 pixel shift on the detector. This is a differential movement from the CCD 1 image so the effect depends on the operating mode. In 2-CCD mode this appears as a static gross tilt error in the Y direction which should be

removed during acquisition. The alignment tolerances are then dependent on second order distortion through relay lens 3, which will be small.

Since we must re-acquire the guide star after changing the beam-splitter, there is no case where we would use the offsets for the 1-CCD mode in the 2-CCD case or vice versa.

4.3. Laser upgrade

This will be achieved via a full aperture lens in the lenslet wheel which is upstream of the WFS camera. The requirements on the camera are to centroid a single spot. Both 1 or 2 CCD modes should achieve this within the specified latency. [A 20x20 window can be read out in 180-350 μ s with 1CCD and 90-125 μ sec with 2 CCD's.]

4.4. Ghosting

The WFS optical design was analysed for ghosting at the PDR. The requirement to keep ghosts to a level which does not affect the centroid process now applies to the whole WFS including the 2CCD optics.

The baseline mode uses a 4x4 pixel grid. Consider the effect of a ghost in the profile as a weighted sum of the star and the ghost as separate elements. The worst case will be with the star centred between the left most pixel pair and the ghost centred on the right most pair. The star and ghost will be approx 2 pixels wide. The separation is thus 2 pixels. Relative to the star, the ghosts influence on the centroid will be given by

$$c_{err} \approx \frac{d * sig_{star}}{sig_{ghost} + sig_{star}}$$

$$sig_{ghost} \approx (d * 1 / c_{err} + 1) sig_{star}$$

where c_{err} and d are in pixels.

For the 4x4 baseline case, the ghost must be fainter than 1/19 of the star to meet an error of 0.1 pixels. For the 8x8 pixel full subaperture case, the ghost must be fainter than 1/60 of the star to meet an error of 0.1 pixels.

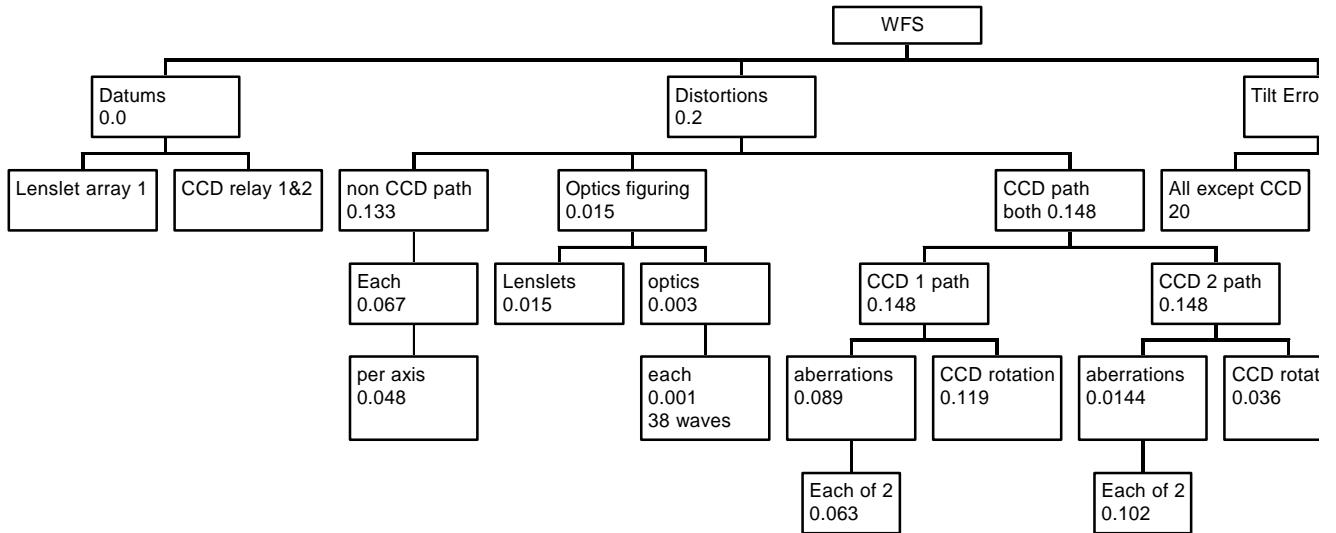
The ghost will add up in phase so for the 10 flat surfaces in the WFS, each needs to be at a level of 1/600 or 0.002 of the star. The difference between 6 and 8 surfaces is not large in the 2CCD architecture.

The requirement is thus that the total level of ghosts in the WFS must be less than 1/60 of the stellar signal, Each element should contribute less than 1/600 of the stellar signal on average.

4.5. Alignment Error Budget - general.

This remains the same as for the WFS as a whole apart from having one more element (the beamsplitter) so the division for specifications. At the time of writing (8/5/97) the detail of the error budget is mostly complete with only a few items unverified.

NAOMI WFS Alignment Error Budget



4.6. Positioning

The 2CCD heads and relay form a camera unit which is identical in function to the PDR camera unit. The camera mounts onto the same focus slide. Thus all positioning requirements except the relay are unchanged from PDR.

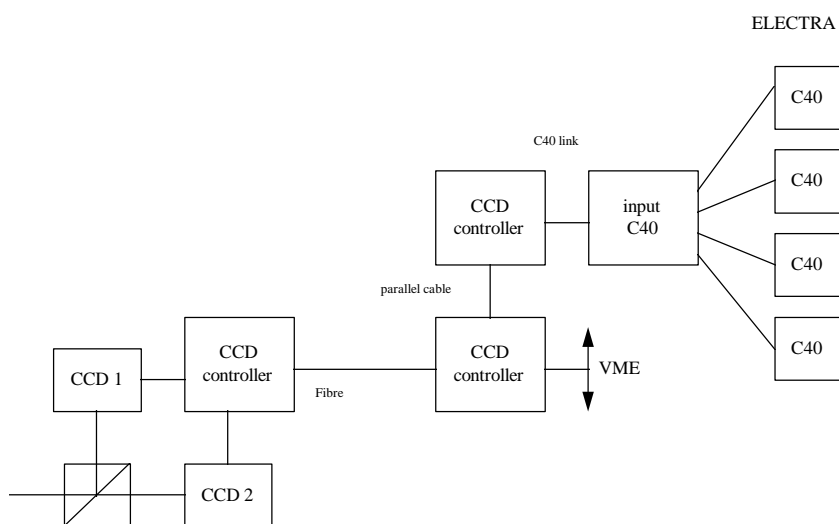
For the relay internals, the one mechanism is the beamsplitter slide.

4.7. Data processing

The WFS is required to provide a feed of raw pixel data to the C40 array in electra which does the centroiding and reconstruction. No data processing is done in the camera. The latency requirement includes the data transfer time and the centroiding process.

The requirement to provide a flexible readout scheme and the goal to provide “on the fly” changes in readout speed and mode imply that attention has to be paid to the methods available for changing readout mode and scheme.

Figure 4-1 2-CCD architecture



5. Hardware Proposal

The following camera system is proposed, to replace the CCD & relay sub -assembly in the WFS as described at PDR:

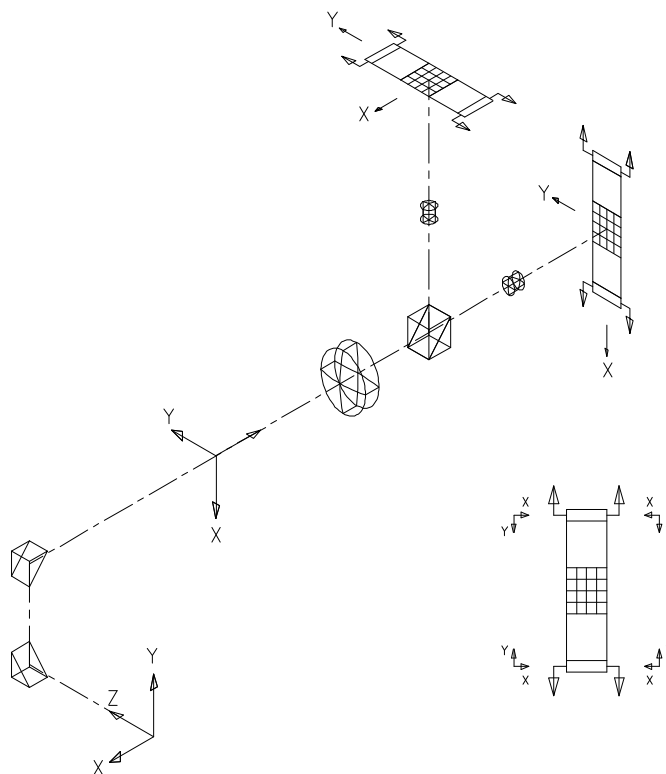
- ?? Shutter. (unchanged from PDR design)
- ?? Relay lens system to re-scale the lenslets to both CCDs.
- ?? 2 CCD39 detectors, oriented orthogonally in the input focal plane.
- ?? Beamsplitter to provide separate focal planes for each detector.
- ?? Compensating optics to provide a straight through path for operation with one CCD

- ?? Remotely operated interchange between the Beamsplitter and the Compensating optics
- ?? Light tight after shutter.
- ?? Individual adjustment of each CCD for x,y,z and rotation alignment.
- ?? Single 8 port SDSU controller to read out both CCD detectors.
- ?? Single data Fibre feed to VME card (second fibre for commands from VME card).
- ?? Parallel data output port containing all output channels.
- ?? Single C40 accepting all 8 channels of data and de-multiplexing to existing electra hardware.
- ?? Frame header containing data format information.
- ?? Synchronous on-line change of readout modes & centroid algorithms.
- ?? Test and debug of CCD operation via standard VME interface
- ?? Control of WFS CCD via Gemini standard interface possible.

5.1. System geometry

Figure 5-2 shows the relative orientation of the various focal plane co-ordinate systems in the WFS. This shows how we arrange to split the beam and orient the 2 CCD's so that one bins vertically in X and the other bins vertically in Y.

5.2. Figure 5-2 Orientation of focal planes in the WFS



5.3. Optical Layout

Figure 5-3 shows a side elevation of the proposed camera system. The beam to the upper CCD head is nominally the same as to the straight through one.

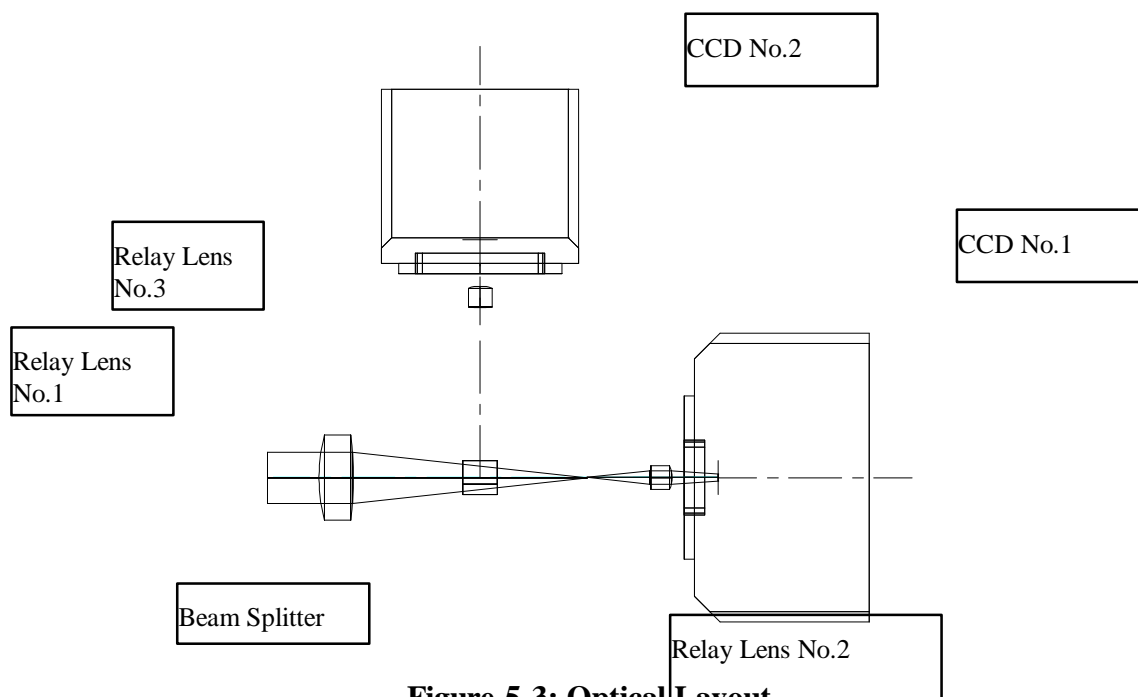


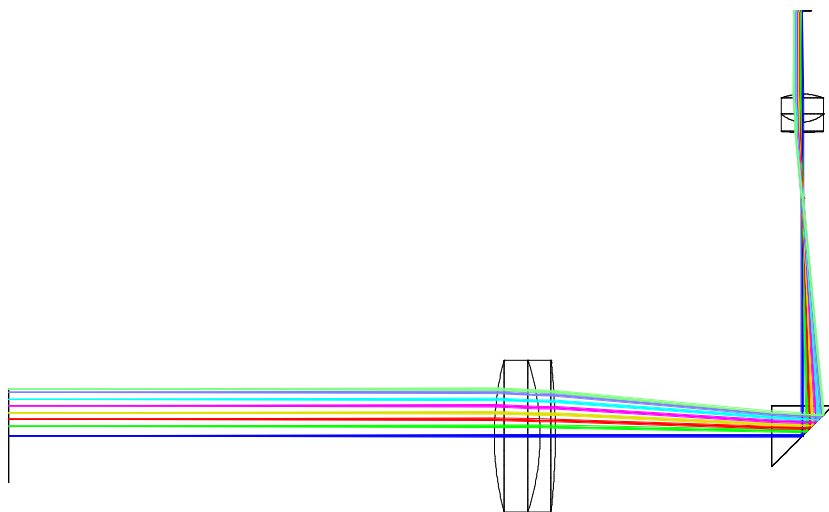
Figure 5-3: Optical Layout

6. Detailed Description

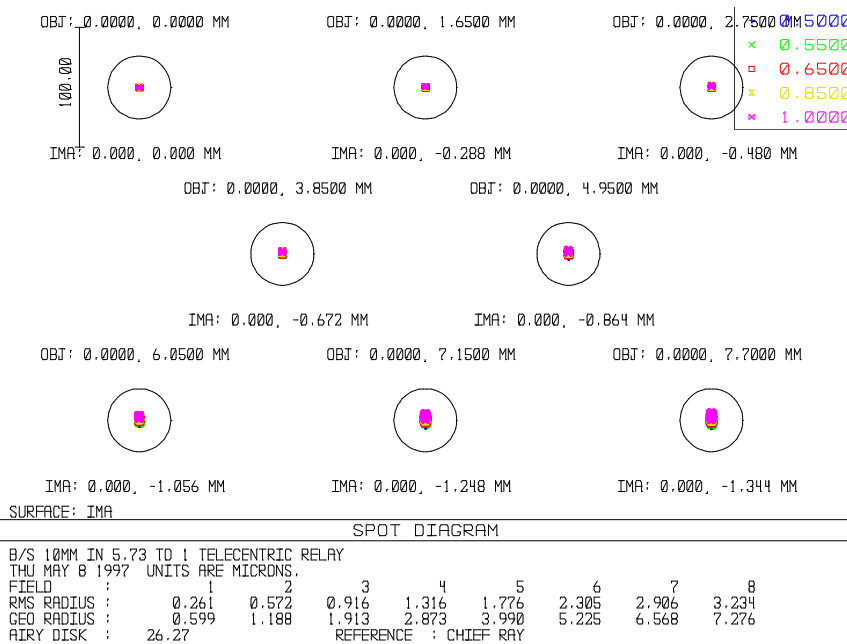
6.1. Optics

6.1.1. Optical design

The wavefront sensor relay design is essentially that described in the WFS PDR (section 4.7) with the addition of a beamsplitter and a second short conjugate re-imaging lens. The distance between the two lenses in the relay has to be adjusted to accommodate the shift in the position of the pupil image introduced by the beamsplitter. If the system is to be used with all the light falling on one CCD, the beamsplitter must be replaced by a compensating plain glass block in order to maintain telecentricity. The layout, including the fold at the beamsplitter is shown below. The spot diagram for this new layout is shown in the accompanying figure.



Folded path of telecentric CCD relay



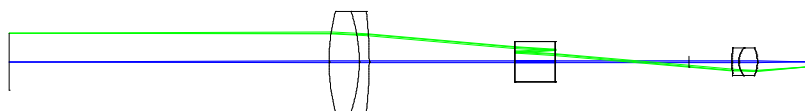
Spot diagram for relay plus beamsplitter

6.1.2. Beamsplitter coating

The beamsplitter coating should be of the hybrid partial reflection type supplied by Melles Griot. This coating has some absorption (10%) but low polarisation, both reflection and transmission are approximately 45% and the s- and p-plane components are within 10% of each other.

6.1.3. Ghosting in the beamsplitter

The beamsplitter lies in the collimated beam within the telecentric relay this will lead to the production of in focus ghosts at the CCD arising from the two reflection path from front and back surfaces of the beamsplitter cube. For off-axis spots the collimated beam walks across the beamsplitter and passes through the lens closest to the CCD at a larger radial distance than the parent spot. This leads to ghosts from off-axis spots being displaced from the parent, having a larger aberration spread and not being telecentric. Although the aberration spread is increased for the ghosts it does not exceed the diffraction spread so that the attenuation is purely that given by the anti-reflection coatings. At the extremes of the wavelength range there is 2% reflection at each surface leading to an attenuation of 4×10^{-4} for the ghost. In the middle of the coating range the attenuation is greater than 1×10^{-4} . The displacements of the ghosts for each lenslet are tabulated below.



Passage of off-axis ghost through CCD relay

Field position of spot	Field position of ghost	Displacement of ghost	Displacement of ghost
mm	mm	μm	pixels
0	0	0	0
0.096	0.096	0	0
0.288	0.286	-2	-0.083
0.480	0.475	-5	-0.208
0.672	0.661	-11	-0.458
0.864	0.842	-22	-0.917
1.056	1.018	-38	-1.583
1.248	1.188	-60	-2.500

Position of ghosts from beamsplitter

The last two rows of the column represent the lenslets used for conjugation in an array of 14x14 sub-apertures. The pixel shifts introduced by these ghosts are well below 0.001 pixels.

6.1.4. Stability Sensitivities

All tolerances relate to the optical axis and are ?

X, Y & Z are in ? m

RX, RY & RZ are in degrees

Component	X	Y	Z	RX	RY	RZ
Relay Lens No.1	2.4	2.4	40	.002	.002	n/a
Relay Lens No.2	2.4	2.4	40	.002	.002	n/a
Relay Lens No.3	2.4	2.4	40	.002	.002	n/a
Beam Splitter	500	2.4	2.4	.005	.005	.005
Compensating optics	500	500	*	0.5	0.5	0.5
CCD No.1	2.4	2.4	35	.1	.1	.05
CCD No.2	2.4	2.4	35	.1	.1	.05
Complete Assembly	13	13	50	.009	.009	.05

Table 6-1: Stability sensitivities

6.1.5. Alignment Sensitivities

All tolerances relate to the optical axis and are ?. All tolerances are provisional and have yet to be verified against the detailed alignment error budget.

X, Y & Z are in ? m

RX, RY & RZ are in degrees

Component	X	Y	Z	RX	RY	RZ
Relay Lens No.1	50	50	100	.05	.05	n/a
Relay Lens No.2	50	50	100	.05	.05	n/a
Relay Lens No.3	50	50	100	.05	.05	n/a
Beam Splitter	100	100	100	.1	.1	.1
Compensating optics	100	100	100	0.5	0.5	0.5
CCD No.1	2.4	2.4	35	.1	.1	.05
CCD No.2	2.4	2.4	35	.1	.1	.05
Complete Assembly	50	50	100	.05	.05	n/a

Table 6-2: Alignment Sensitivities

6.2. Mechanical Assembly

The complete assembly, as shown in drawing BN033, is attached to the carriage of the main linear bearing of the WFS system as previously described in the PDR documentation.

A bridge structure supports the two Gemini style CCD heads at 90 degrees to each other and also provides the mounting for the Relay lens systems.

The Beam Splitter and Compensating Plate are mounted to a two position linear slide.

The complete system is enclosed in a light tight cover with an electronic shutter fitted in front of the first relay lens.

Adjustments are provided to centre the two CCD heads and the third relay lens. These are made once only during initial set-up and then locked in position. The setting jig used for the CCD head is intended to be removed after use. Adjustment and alignment operations should only be performed by suitably experienced engineers/technicians.

The Detector Controller is fixed to the WFS baseplate and the cables and coolant hoses will be guided through a flexible cable chain to accommodate the linear movement of the slide.

6.2.1. Slide Carriage/Baseplate

Precision machined to provide a well defined datum for the detector unit with respect to the main WFS linear slide.

6.2.2. Bridge Structure

Fabricated from aluminium alloy with accurately machined datum faces to register with the baseplate and the relay lens barrel.

6.2.3. Relay Lens Nos. 1 and 2

These will be supplied by the lens manufacturer, assembled and mutually aligned within a purpose built barrel mount.

Centring achievable $\pm 10 \mu\text{m}$

Tilt achievable $\pm .050^\circ$

The barrel will be accurately located in the supporting bridge structure by a precision registration diameter.

This assembled lens, when mounted in the bridge structure, will be used to set the optical axis datum for the remainder of the sub-system. Appropriate targets and lasers will be required to mark this axis during set-up.

6.2.4. Relay Lens No. 3

Relay Lens No. 3 needs to be adjustable to permit the correct alignment to the folded beam.

Range of adjustments provided: -

XY $\pm 1.0\text{mm}$ - use M3 x 0.5 screws to centre lens cell in support structure this will give centring to $\pm 10 \mu\text{m}$ (1/50th of a turn, 7.2°)

Z $\pm 1.0\text{mm}$ - shim/machining required adjust on assembly. This will give adjustment to $25 \mu\text{m}$

Tilt: not adjustable.

6.2.5. Beam Splitter

Mounted to a THK HSR151UUC1+160L linear slide and driven by a Digital Linear Actuator - McLennon Servo Supplies L92111-P1 (similar to type used on ISIS and WYFFOS).

Datum Switches are provided to encode the slide position, IN or OUT.

Positioning possible by machining only (no adjustments to BS), the below figures contribute to the range of adjustment required by Relay lens No.3

X - controlled by linear slide

Y - height ? 100 ?m

Z - ? 100?m

Tilt - ? 0.10?

Slide Repeatability for Beam Splitter

X: stepper motor step size of 25 ?m.

Y - ? 2 ?m

Z - ? 2 ?m

RX - ? .005? (18")

RY - ? .005? (18")

RZ - ? .005? (18")

6.2.6. Compensating Optic

Plain glass to replace beam splitter and permit the use of CCD No.1 in a straight through mode.

It is attached to the BS slide and so will be the same as the BS.

6.2.7. CCD Nos. 1 & 2

Each detector, as shown in DAO drg. GWD0001, is identical and the design uses common components to mount to the bridge support structure. To centre the lens, both detectors are adjustable in X, Y, Z and RZ. All adjustments are designed to be for alignment purposes only and then "locked".

6.2.7.1. Rotation RZ

Provided by mounting the CCD to a plate that has a central pivot. Adjustment is by a tangent arm with M3 x 0.5 screws acting at 50mm radius.

$0.5/50 = 0.01$ per turn of screw

Alignment possible to 0.05 ? (1/10th of a turn of screw)

6.2.7.2. Translation X and Y

One off setting up adjustment to be operated by a suitably experienced engineer/technician. Differential micrometers are mounted in a setting jig. This jig secures to the support structure and by using the micrometers the CCD front mounting plate can be pushed in X and Y to provide the required centring. Spring pressure is used to support the mass of the CCD head (approx. 0.6kg).

Range 2mm

Resolution 1 ?m

When centring is complete the assembly is finally locked in position using the clamp screws and the Jig removed.

The same jig is used for both CCD Heads.

6.2.7.3. Tilts RX and RY

Not adjustable.

Assembly Accuracy ? 1?

6.2.8. Detector Controller

This is a relatively large and heavy unit (approx. 340 x 200 x 140mm and 8 kg). It is intended to fix this to the WFS baseplate, separate from the slide. The cables and hoses from the controller to the detector will be supported in a plastic cable chain to accommodate the required 300mm of travel, whilst keeping the cable length to a minimum (nominal 500mm).

Should the cabling requirement change, the CCD controller could be mounted on an outrigger of the CCD camera focus carriage, or on a separate slide slaved to the camera focus position.

6.2.9. Shutter

A Prontor type E40, will be used to provide a fast acting remotely operated electronic shutter. This is mounted in front of the first relay lens. Modifications will be required to incorporate position sensing switches and a magnetically latched solenoid. The latching solenoid will enable the power to be switched off when holding the shutter open, thereby removing a potential heat source near the optical path.

6.2.10. Complete Camera Assembly

The whole sub-assembly, when internally aligned, is mounted to the main linear slide of the WFS system.

Adjustments X, Y, RX, RY and RZ can be achieved using shims or by final machining after measurement of the positional and tilt errors.

25? m smallest adjustment to height.

With a fixing screw baseline 150mm approx, this gives 0.025/150 ? 0.01? tilt.

Although the sub-assembly will have been fully assembled and aligned “off -line”, it may be necessary to provide final “tweaking” to the CCD heads for alignment to the SH spot arrays. This will be done using the CCD adjusting mechanisms in X, Y and RZ.

6.2.11. Mass

Table 6-3 gives the mass estimates for the individual components of the system.

Table 6-3 Component Masses

Component	Mass
2 off CCD head @ 0.6kg each	1.2
Relay Lens and Barrel	0.15
2 off Centring plates @ 0.15kg each	0.3
2 off Rotation plates @ 0.1kg each	0.2
1 off shutter	0.1
Support Structure	1.0
Cables & Hoses	0.25

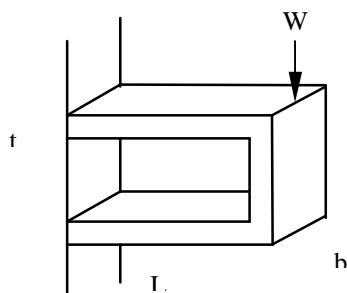
Total

3.2

6.2.12. Stability

6.2.12.1. Stiffness of Structure

A first order approximation of the stiffness of the structure can be made using a simple cantilever beam calculation.



$L = 100\text{mm}$
 $t = 10\text{mm}$
 $b = 140\text{mm}$
 $E = \text{Young's Modulus} = 71 \times 10^3 \text{ N/mm}^2$
 $W = 30\text{N}$

The load of 30 N is a worst case assumption that all the load acts at one point.

The direction of load is along the optical axis Z which is only valid for external acting loads to system. E.g. Telescope acceleration or Vibration. To achieve the value of 30N used in the calculation the acceleration must be equivalent to 1g (highly unlikely).

$$\text{Deflection} = \frac{WL^3}{2Ebt^3} = \frac{30 \times 100^3}{2 \times 71 \times 10^3 \times 140 \times 10^3} = 1.5 \times 10^{-3} \text{ mm} (1.5 \mu\text{m})$$

Formula from SIRA Optomechanical Design Course Notes (Flexures) and Case 17 Machinery's Handbook.

$$\text{Stiffness}(k) = \frac{\text{load}}{\text{deflection}} = \frac{30}{1.5 \times 10^{-3}} = 20 \times 10^3 \text{ N/mm} (20 \times 10^6 \text{ N/m})$$

$$\text{Natural Frequency}(f) = \frac{1}{2\pi} \sqrt{\frac{k}{m}} = \frac{1}{2\pi} \sqrt{\frac{20 \times 10^6}{3}} = 410.9\text{Hz}$$

6.2.12.2. Bearing Rigidity for Beam Splitter Slide

THK HSR 15 linear bearing

Assumed value of $k = 0.05\text{kN/m}$ (based on values of .04 for HSR8 and .065 for SR20)

Load acting on bearing approx. 1N (0.1kg)

$$\text{Natural Frequency}(f) = \frac{1}{2\pi} \sqrt{\frac{k}{m}} = \frac{1}{2\pi} \sqrt{\frac{0.05 \times 10^9}{0.1}} = 3.55\text{kHz}$$

6.2.12.3. Thermal Stability

From information provided the maximum temperature gradient = 1 °C/hour

Coefficient of thermal expansion for Aluminium = $23 \times 10^{-6}/^{\circ}\text{C}$

Coefficient of thermal expansion for Steel = $13 \times 10^{-6}/^{\circ}\text{C}$

In the twin head CCD system all components are manufactured from Aluminium with the exception of the steel linear bearing for the beam splitter interchange. This bearing has a height of 28mm.

Differential thermal expansion is limited to that occurring over this distance

For a 1°C temperature change the differential expansion is: -

$$28 \times 1 \times (23-13) \times 10^{-6} = 0.28 \times 10^{-3} \text{ mm (0.28 } \mu\text{m)}$$

This would equate to a decentre of the image at the CCD.

6.2.13. Possible Future Conjugation Upgrade

It should be possible to replace the baseplate assembly with a motorised linear XZ slide assembly. The approximate mass of 3kg would indicate that a small scale readily available slide would be suitable, e.g. Physik Instrumente M125 XZ

A spacer will be left between the focus carriage and the camera baseplate for this to be implemented. This will be at least 25 mm thick.

6.3. Alignment and integration

The WFS concept as a whole is unchanged so aligning the rest of the system is not affected, using the straight through CCD. The alignment of the beamsplitter in angle will affect the position of the beam on CCD 1 but only to second order. The sensitivity to tilt error for the beamsplitter onto the CCD2 is tight, as it is downstream of the lenslet array and differential from CCD to CCD. 0.004 degrees of tilt gives an 0.1 pixel offset. Since there is a very small space available to implement an adjustable mount, we have based the design on a fixed, non adjustable beamsplitter which defines the datum for the CCD2 beam, we expect the non repeatability to be about 0.1 pixels on the CCD and will be taken out via an offset in 4x4 mode. The 2CCD configuration is not expected to be used with Quadcell readout mode.

6.3.1. Relay lens no.1 to relay lens no.2

The mounting of these two lenses into a machined barrel will be undertaken by the optical manufacturer. The optical axis defined by these two lenses provides the datum to which the beamsplitter, compensating optics and third relay lens must be aligned. The optical axis of the relay can be found by aligning a laser on the centre of the lenses. The light back-reflected from the spherical surfaces of the lenses forms a set of interference rings. Tilt of the assembly leads to a shear of the different interference patterns and lateral translation produces a non uniform illumination of the pattern. With the radius of curvature present in the relay design, a laser and target set at 500mm from the relay will provide the required accuracy for the determination of the alignment axis with a minimum displacement at the target of 1mm.

6.3.2. Beamsplitter slide

The relay lens barrel mount and the slide are mechanically assembled and the gross alignment of the beamsplitter and compensating block is carried out by machining their individual mounts. The slide will be used at two positions, one for the beamsplitter and the other for the compensating block. The beam splitter and compensating block are checked for squaring on, to the laser beam using the back reflection techniques outlined above. The height adjustment of the beamsplitter is achieved by machining to bring the folded axis into the range of adjustment available on lens 3 and the CCD mount. Orthogonality of the folded axis to the lens mounting face can be checked by back reflection from a small mirror supported on the lens mounting surface using two measurements taken with the mirror rotated through 180° about the Z axis.

6.3.3. Lens 3

This lens is brought onto the folded axis and aligned using back reflections, the return beam from lens 2 is blocked off during this operation.

6.3.4. CCD Nos 1&2

The adjustments provided for these two CCDs allow them to be brought into registration with the spot pattern produced by the lenslet array. A mutual alignment can be achieved off the main WFS assembly using a simple three hole mask but the final check must be made after the CCD relay optics have been integrated into the WFS.

6.3.5. Alignment of CCD relay to WFS optical axis

The relay is aligned using the 'straight through' configuration with the compensating block in place. The targetry set up to define the WFS optical axis is used to provide the datum for a laser alignment procedure as used in the sub-assembly. The relay is brought into alignment with the collimator, the lenslets are deployed and the two CCDs are checked for rotation and displacement.

6.4. CCD Controller and software

The proposed CCD controller is the SDSU controller which has recently been adopted as the new ING standard. Its capabilities are summarised in Table 6-4. It is used in the following other AO related projects:

?? Steward Observatory AO system WFS.

?? Gemini PWFS.

Table 6-4 SDSU controller parameters

CCD head architecture	Gemini PWFS head on cable. sequence generated in software by 50Mhz DSP in timing board. 40 ns sequence period. One clock board per CCD for ccd clock driving. One signal board per port pair.
signal board details	accepts 1 or 2 channels, 1 Mhz max sample rate CDS sampling. 16 bit ADC
channels	up to 32.
data transfer	pixel multiplex sent via fibre to DSP in receiver board. 50 Mbit fibre available, speed upgrade to 200 Mbit planned. 4 channel txfer time 1.28 μ s 8 channel txfer time 2.56 μ s
data word length	16 or 24 bit selectable.
control	commands sent from receiver board DSP via fibre.
data acquisition	VME card or Sbus card with DSP which has VMEbus master capability. New board design has parallel data port.
Readout sequencing	Entirely software driven by timing board DSP. A mode can be a single directly coded subroutine or parameters to control a generic routine.
Flexible readout switching	The readout modes may be switched by sending a command to call a different subroutine. Limited by DSP memory to about 2 schemes at one time.
Head unit size	58x85x55 mm
Cable length to electronics rack	0.5m
Electronics Rack size	140x172x343 mm
Power supply rack size	230x200x110 mm
TE cooler PSU size	250x88x124 mm
Max distance from camera to Acquisition system rack	< 20m (parallel) < 100m (fibre-optic)
CCD	EEV CCD39 or CCD42
Cooling system	Integral T.E. cooled CCD package

Heat removal	CCD housing cooled by glycol/water circuit CCD rack cooled by TBC
Max pixel rate	1 MHz planned, 0.5 MHz demonstrated
Sampling technique	CDS
Read noise vs. speed relationship	Noise goes down with slower readout. 8.8 erms demonstrated at 500 kHz rate. DAO new video board prototype demonstrated to meet the Gemini PWFS spec of: 3.4 erms @ 500 kHz, 2.2 erms @ 100 kHz
dwll time between frame readouts	100 ?sec
Binning available	yes
Windowing available	yes
on the fly change of readout waveforms	yes
on the fly change of integration time	yes
frame sync method	header sent with each frame. Identifies readout sequence.
Data output format	Fibre-link or parallel bus
Data acquisition hardware	DSP receiver board to VME bus with parallel output port. DSP receiver board to Sbus Parallel interface card to PCI bus

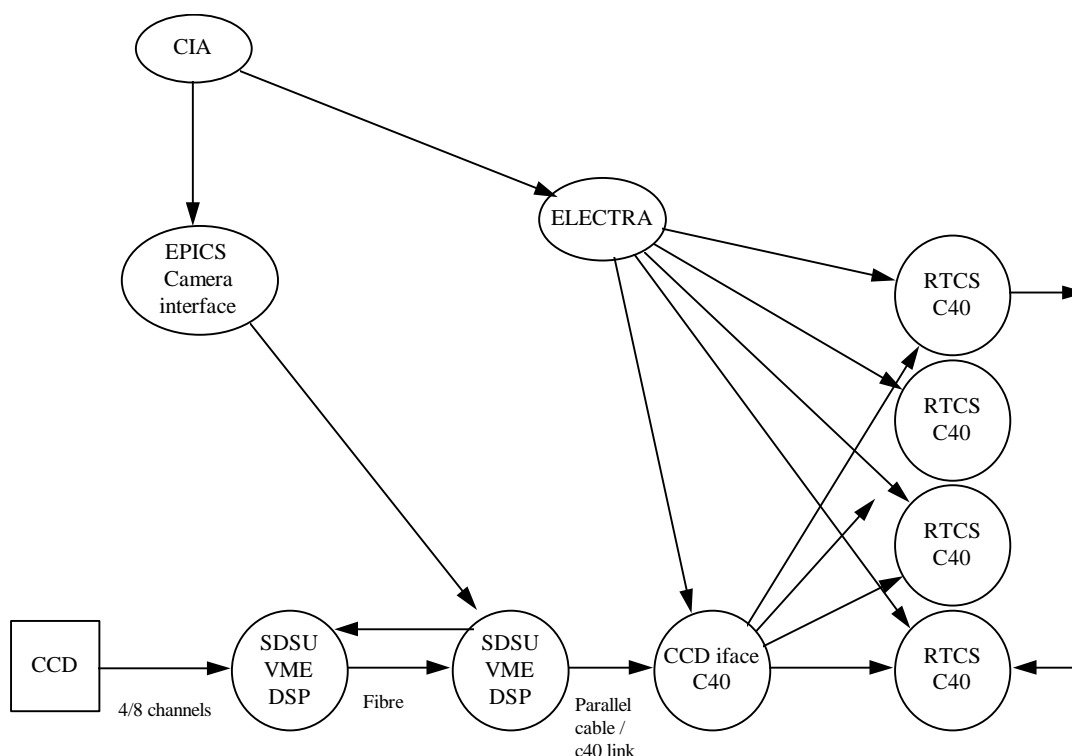
The fibre bandwidth is the current bottleneck. The latency calculations are done on the basis of 12 bits per word, which will require small modifications to the timing and receiver boards. The standard hardware uses 16 or 24 bits. For the case where the 12 bit system reads out in 296 ?s, moving to 16 bit words would increase the frame time to 330 ?s.

These are obviously simulations. Should the latency be found to be too large with the delivered system, then the following upgrades could be considered:

- ?? Increase the fibre speed - this is planned anyway and will remove the need to modify the boards ourselves.
- ?? Add a second controller which will double the fibre bandwidth. A design is being developed to synchronise two of these controllers as a separate project for ING.

The data appears on the parallel cable at one 16 bit word every 320 nsec. [6.25 Mbyte/sec] Should the single C40 link not be found to be fast enough, a simple hardware multiplexer could be built which would provide input on multiple C40 links. It would need some intelligence to demux the data and not the header information.

The high-level control of this camera is being implemented for several different projects and the requirements are extremely unstable at the present time. Only the lower layers are of relevance to this discussion.

Figure 6-1 Processor Data flow diagram

To predict the latency for different CCD cameras with various readout modes, the readout process was modelled in a spreadsheet. The results are summarised in Appendix C. This model has been independently verified.

For the single CCD 4 port SDSU camera, it could read the baseline mode in 488 μ s and the quadcell mode in 165 μ s. With 2CCD's the 8 port SDSU could read the baseline mode in 248 μ s and the quadcell in 125 μ s. These timings assume 12 bits/pix and very fast skipping times. A more realistic scenario is based on timings used in existing cameras and gives the following times:

Mode	4 port 1 CCD time μ s	8 port 2 CCD time μ s
Baseline 4x4	523	300
Quad-cell	201	182

6.5. Frame data packets.

One significant advantage of this architecture is that since the data from the CCD passes through the DSP which generates the sequence, we can add header information to the ccd data frame to indicate the readout mode, data length and other information to allow automatic synchronisation of the pixel processing routine with the ccd data. A proposed packet structure is shown in Figure 6-2 and is proposed for discussion. It is described in detail in Appendix 2

Figure 6-2 CCD data packet protocol

6.6. Detector

We propose to use the Gemini PWFS detector head, which is used with this controller to read out a CCD39 from EEV. Drawing GWD0001 shows the assembly of the head.

there are two versions of this chip, IMO (aka MPP) and standard. The IMO version is optimised for low dark current. The difference is a factor of order 100.

Discussions with EEV have ascertained that there are difficulties sourcing the IMO version, which Gemini PWFS uses. There are unlikely to be wafers available for delivery within the next 10 -15 months. Standard devices are available now.

It is not clear that the IMO version is needed for NAOMI as we do not intend to operate the WFS with integration times of the order of seconds, so we are not expecting dark current to be a problem.

We will review the situation in a few weeks time after we have decided which version of the CCD to use. It looks like the non IMO version should be acceptable. In that case, we should be able to procure the CCDs about 6-8 weeks after order.

EEV have not yet succeeded in constructing a complete evacuated CCD + peltier + hermetic seal for the Gemini heads. We will review whether we need a head built to the same standards. We have the advantage of following Gemini in this area so that we can use whatever solution they discover.

7. Interfaces

7.1. Optical

The camera re-images a field 15.4 mm square with a pixel scale of 0.1375 mm/pix. The focal plane is 80 mm in front of the nominal centre of the first relay lens and nominally 100 mm above the focus slide carriage. Each CCD sees the same image.

7.2. Mechanical

7.2.1. Interface to remainder of WFS System

The relay lens, beamsplitter and 2 CCD detectors are assembled to create one module. This module is attached to the carriage of the WFS linear bearing system.

7.2.2. CCD Detector Interface

Provision must be made to accommodate the following: -

- ?? 2 off CCD Detector Head
- ?? 1 off Detector Controller
- ?? 1 off Power Supply Unit - CCD Controller
- ?? 2 off Power Supply Unit - T/E Cooler
- ?? Circulating Coolant Supplies

Mechanical interfaces to the above are described in: -

Gemini ICD 1.6.1/1.6.2 A&G Opto-Mechanical Subsystem to Wavefront Sensor Subsystem.

Drawing 90-RGO-0007-0016 shows the physical dimensions and mounting details of the CCD head.

It should be assumed that the Detector Controller must be located close to the CCD head whilst the power supply units will be situated in the control electronics enclosure.

7.3. Electrical

7.3.1. Interface to WFS System

Functions requiring an electrical interface are: -

- Drive Motor - Beam Splitter interchange slide

Position ID switch - Beam Splitter interchange slide - 2 off (in or out)

Shutter Actuator (solenoid)

Position ID switch - Shutter - 2 off (open or closed)

7.3.2. CCD Detector Interface

Electrical interfaces are described in Gemini ICD 1.6.1/1.6.2

7.4. Software

The software design for SDSU control for the rest of ING will be followed. It is likely that the camera control interface will use the SDSUlib vxWorks C library developed for Gemini. This has an EPICS layer above it to provide functionality via the Gemini CAD CAR records. A data flow diagram for this can be seen in Figure 6-1 This shows one possible route for controlling the camera.

8. Cost and procurement issues.

A summary of the cost of the system with the 2CCD option compared with the PDR costing is shown in Table 8-1. The incremental cost of the 2CCD system is £16.5k which is more than offset by the fact that the CCD camera is now a stable existing item which does not require significant upgrade costs to be budgeted for. The net saving in capital is £20k, which is offset by an increase in effort of 107 days in the current plan.

There are several areas of work which are ill -defined at present, especially in the embedded software to run in the camera and the infrastructure for controlling the camera. Please expect effort requirements to rise as these are evaluated and clarified.

Another area of uncertainty in the costing is the actual hardware to be purchased for the SDSU camera. We do not know how many spare boards will be needed, or whether a complete spare camera will be needed. A trade study will be carried out shortly to identify the compromises. This does not affect the logic of this proposal.

Table 8-1 Capital cost summary of WFS with 2CCD option.

NAOMI WFS costing							19/05/97		
							Version 3.0		
WFS details	Optics	Mechanics	electronics	CCD hardware	Other	total	@ PDR	diff	
WFS Pick-off	3,248	1,595	1,820			6,663	6,108	555	
WFS Fore-optics	14,990	4,270	2,800			22,060	22,060	0	
WFS CCD & relay	2,439	4,815	919			8,173	3,403	4,770	
WFS chassis etc		8,185				8,185	8,035	150	
common to WFS	2,433	29,325	13,476		2300	47,534	37,301	10,232	
RGO integration					4,633	4,633	3,900	733	
subtotal exc cal source	23,110	48,190	19,015	-	6,933	97,248	80,808	16,440	
WFS Cal source	2,643	640	30			3,313	3,207	106	
WFS total	25,753	48,830	19,045	-	6,933	100,561	84,015	16,546	
	Optics	Mechanics	electronics	CCD hardware	Other	total			
system design to date						2500	2,500	-	
JOSE						7500	7,500	-	
system engineering						7,500	7,500	-	
Software & controls						14,200	14,200	-	
WFS	25,753	48,830	19,045	-	6,933	100,561	84,015	16,546	
CCD camera				54,233		54,233	90,700	- 36,467	
commissioning					14100	14,100	14,100	-	
project management					9600	9,600	9,600	-	
						-			
total	25,753	48,830	19,045	54,233	62,333	210,194	230,115	- 19,921	
@PDR	26,146	37,910	14,259	90,700	61,100	230,115			
diff	- 393	10,920	4,786	- 36,467	1,233	- 19,921			

Procuring the CCD and controller for the 2 - CCD route will not be significantly different than the 1 - CCD route, but going for a conventional controller like the SDSU makes the technical risk much less so the estimates are better.

Correct operation of the camera is important for correct operation of the WFS. Optimising readout of the CCD39 is critical to achieving the performance specifications of the WFS so we need the camera to be available for optimisation in good time. In the event of the CCD performance not being up to expectations, we also wish to have as much slack as possible to fix the problem. Since the camera can be fed with standard bench mounted optics for testing, the camera subsystem can be built and integrated early in the plan, with the rest of the WFS added as it becomes available. This could allow preliminary integration of the CCD camera with the ELECTRA rack whilst the rest of the WFS is being built.

We therefore propose to start procuring the CCD and camera as soon as possible after approval of this proposal. We will decide on CCD mask type and packaging options to follow the Gemini head standard, once that design is ratified.

Recent indications from Bob Leach are that we should have no problems with delivery timescales for controllers at the moment. We ought to order the controller before this situation changes, and also to include it in the bulk order which RGO is placing for ING at this point in time.

Appendix 1. Document history

Version 0.1 -0.3 - internal first drafts

Version 1.0 - released to project. 21/5/97 abg,spw,ajw

Appendix 2. CCD data packet protocol.

Introduction

The CCD data read from the SDSU controller is generated by a DSP and a frame packet is sent to a C40 within the ELECTRA system. A frame packet protocol is proposed which defines a header to be appended to the CCD data which will allow identification and decoding of the different readout modes and synchronisation of the receiving process to the transmitting process. This is summarised in Figure 8-1

Physical Layer

This will be via a single fibre optic link from the Timing board in the Camera rack to the VME interface board in the Electra or dedicated rack. Parallel digital data will be output on a plug to an interface card which converts this to a C40 link which runs to a single data reception C40.

Serial data word packet format

This applies to the data on the SDSU timing to VME interface board fibre.

Each word will be in serial format, with a '1' start bit followed by N data bits, MSB first.

12 bits per word will be used in the base line system.

16 or 24 bits per word can be configured, and will save cost at the expense of latency.

The serial data is continuously clocked and the data stream is packed with '0's in between data words.

Parallel data word format.

This applies to the VME interface to C40 link interface.

Connector: TBC

Signal type: TBC

Connector pinout: TBC

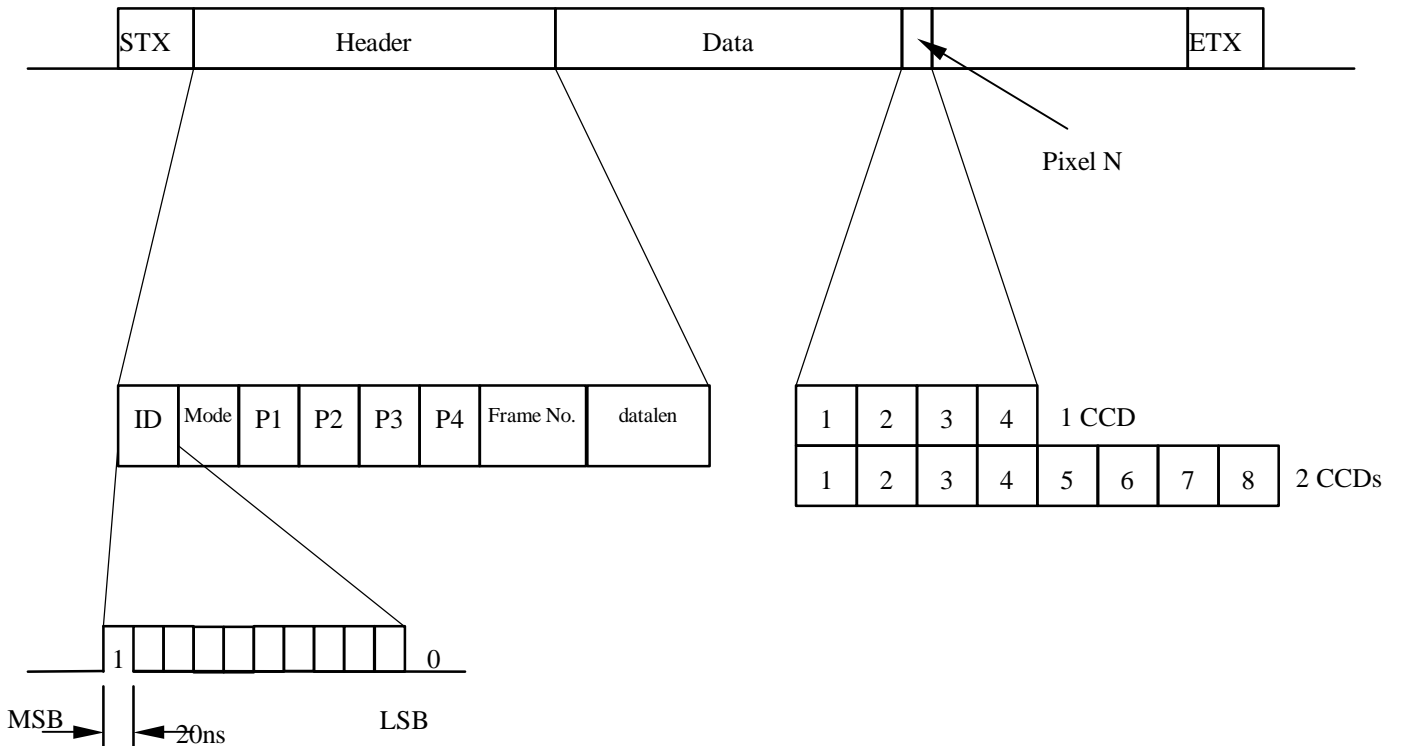
Data codes

The CCD controller electronics will be adjusted to put the zero point of the ADC at above 0x100 to leave the bottom 256 data numbers free for signalling code s.

Table 8-2 Data codes

Data number	Mnemonic	Description
0x000-0x07f	header data	7 bit data.
0x82	STX	start of transmission: frame start
0x84	ETX	end of transmission: frame end.
0x80,0x81,0x83,0x85-0xff	Reserved	
0x100-0x3ff	CCD data	CCD data

Figure 8-1 CCD data frame



Frame packet structure

Each frame will be structured as shown below:

Table 8-3 Frame packet structure

Word number	Name	description
1	STX	Start of packet flag, used to detect when valid data begins. Can trigger flush of previous frames data in case of missing data.
2	ID	controller ID, to facilitate routing if needed. CCD1&2 = 0x10
3	Readout mode	Mode plus 4 accompanying parameters. P1-P4
4	P1	No of pix or subaps in X
5	P2	No of pix or subaps in Y
6	P3	Offset in X (pix or subaps)
7	P4	Offset in Y (pix or subaps)
8	Frame Number	Circulating frame counter:
9	Datalen	Number of words in data section.
10-Datalen+9 inclusive	Data	see table Table 8-4 for details of format of pixels and channels.
Datalen+10	ETX	End of packet marker.

Table 8-4 Frame packet Data section format

packet address	Pixel	channel		Pixel	channel
	8 Channel			4 Channel	
10	1	1		1	1
11	1	2		1	2
12	1	3		1	3
13	1	4		1	4
14	1	5		2	1
15	1	6		2	2
16	1	7		2	3
17	1	8		2	4

18...	2	1		3...	...
19	2	2			
20	2	3			
21	2	4			
22	2	5			
23	2	6			
24	2	7			
25	2	8			
26...	3...				

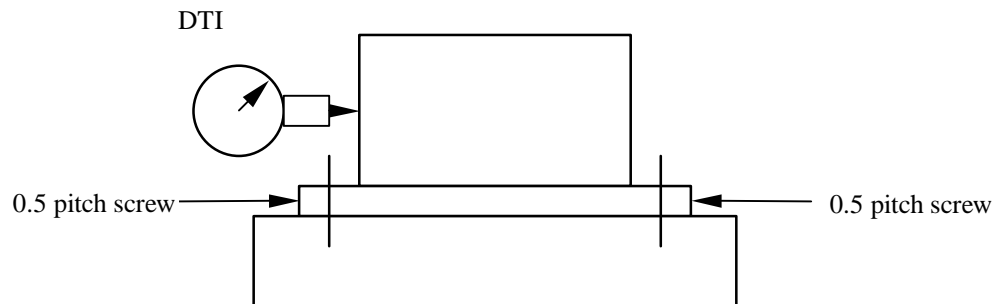
Table 8-5 CCD readout modes

Mode	Name	P1	P2	P3	P4
0	Full frame	Xpix	Ypix	0	0
1	Single window [args in pixel units]	Xsize	Ysize	Xorigin	Yorigin
2	8x8 pix per subap [subap args]	Nx	Ny	Xorigin	Yorigin
3	6x6 pix per subap	Nx	Ny	Xorigin	Yorigin
4	4x4 pix per subap	Nx	Ny	Xorigin	Yorigin
5	1 pix quadcell 2x2 pix per subap in 2x2 box	Nx	Ny	Xorigin	Yorigin
6	4 pix quadcell 2x2 pix per subap in 4x4 box	Nx	Ny	Xorigin	Yorigin
7	9 pix quadcell 2x2 pix per subap in 6x6 box	Nx	Ny	Xorigin	Yorigin
8	16 pix quadcell 2x2 pix per subap in 8x8 box	Nx	Ny	Xorigin	Yorigin
9-0x7f	available for upgrade.				

Appendix 3. Simple Test to prove alignment operations

XY Positioning of CCD Head

Using a model of the Gemini (DAO) CCD Head I mocked up a test to prove the resolution for the positioning mechanism.



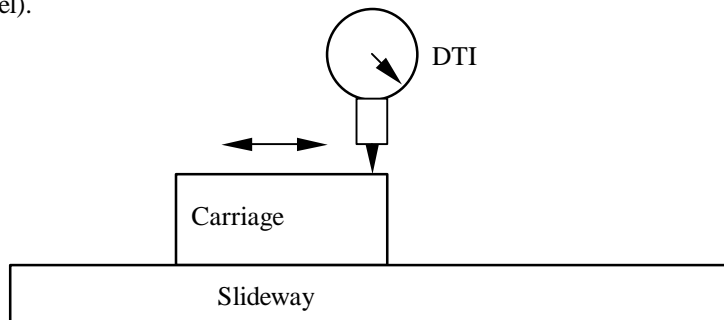
By adjusting one screw against the other it was possible to position the CCD head with a resolution of $2\ \mu\text{m}$ measured on the Dial Test Indicator (DTI). The $2\ \mu\text{m}$ equates to 1/5th of a division on the DTI and is about the limit for the readout resolution and for the resolution of the adjusting screws.

$$\frac{.002}{0.5} \times 360 \times 1.44 \times \text{Rotation of the screw}$$

The intention for the real system is to use Differential micrometers with a resolution of $0.1\ \mu\text{m}$. Therefore I can be confident that the CCD Head can be adjusted for centring to the level of $1\ \mu\text{m}$.

Repeatability of BS Slide

Using a THK slide, model 2RSR12WVMI +320M, as a test for repeatability in X and Y (Z focus = direction of travel).



By moving the slide against two stop positions over a 25mm travel the runout and non-repeatability were measured by the DTI.

Within the measuring capabilities of the DTI no displacement of the DTI was noticed.

Repeatability $\approx 2\ \mu\text{m}$

Tilt $\approx .002/24$ (width of rail) $\approx 0.0047\ \mu\text{m}$

This would indicate that the slide is capable of the required degree of repeatability for the two discrete positions required by the Beam Splitter Slide.

The slide tested is not a precision grade slide and was also of a normal clearance grade, i.e. not pre-loaded to remove any play.

If this slide, that is not designed for precision movement, can provide repeatability of/or near the level required for the BS slide then I have every confidence that a more precision grade version will be even better.

To provide confirmed figures for this application THK have suggested that we purchase, on sale or return, the slide we require. We can then manufacture the system and test it to prove the performance. The test would be based on a simulation of the relay lens system and beam but using a higher magnification (approx. 5x) to give us a higher resolution. A CCD camera would be used to measure the repeatability of the image as the beam splitter is moved out and back.

Appendix 4. SDSU readout time estimates

A spreadsheet¹ was used to model the actual readout sequence, allowing effects like pipelining to be included, using the actual CCD and controller parameters expected.

Table 8-6 Timings for the SDSU camera

scenario #	1	2	3	4	5	6	7	8	9	24	25
name	4 port 12 bit fastest	4 port 12 bit	4 port 16 bit	4 port 12 bit best read noise	8 port 8 bit	8 port 12 bit standard	8 port 12 bit fastest	8 port 12 bit best read noise	8 port 16 bit	8 port sdsu via LVI with status check	8 port sdsu via LVI without status
pix time	1.28	1.28	1.60	1.28	1.92	2.56	2.56	2.56	3.20	3.70	2.40
sample time	1.00	1.00	1.00	1.28	0.86	1.28	1.00	2.56	1.60	3.70	2.40
hclock	0.24	0.32	0.32	0.32	0.32	0.32	0.24	0.32	0.32	0.30	0.30
vclock	0.24	0.88	0.88	0.32	0.88	0.88	0.24	0.32	0.88	0.90	0.90
reset time	0.24	0.32	0.32	0.32	0.32	0.32	0.24	0.32	0.32	0.30	0.30
2D readout (full frame)											
10x10 subaps all pix	2096	2134	2646	2112	3158	4182	4144	4160	5206	6004	3924
2D readout (8x8 subapertures)											
8x8 subaps all pix	1425	1490	1818	1463	2145	2801	2736	2774	3456	3960	2629
6 x 6 pixels in box	896	1011	1164	979	1325	1694	1616	1716	2063	2392	1643
4x4 pixels in box	488	598	659	562	690	869	777	890	1018	1205	872
4 x 4 big pixels	407	541	552	506	634	797	735	833	961	1152	820
2 x 2 big pixels	165	252	254	211	239	280	220	293	321	401	318
1D readout (8x8 subaps)											
8 pixels in X	204	260	301	218	342	424	368	381	506	570	403
6 pixels in X in box	209	286	311	243	338	400	329	366	461	514	389
4 pixels in X in box	176	255	270	212	278	323	248	294	360	405	322
4 big pixels in X	124	199	201	156	222	263	206	238	304	352	269
2 big pixels in X	98	168	169	125	162	182	125	166	203	243	202

Note that all timings are in μ s.

Table 8-7 Timings for Quad Cell readout

scenario #	15	16	17	18	19	20	21	22	23
name	case A	case B	case C	case D	case E QC 1ccd	case F QC 2CCD	case G QC 1ccd fast	case H QC 2CCD same time as G	case I QC 2ccd fast
pix time	3.84	0.50	3.53	0.50	2.04	5.41	1.28	3.87	2.56
sample time	3.84	0.50	3.53	0.50	2.04	5.41	1.28	3.87	2.56
hclock	0.23	0.23	0.30	0.30	0.32	0.32	0.30	0.30	0.30
vclock	0.23	0.23	0.30	0.30	0.88	0.88	0.30	0.30	0.30
reset time	0.23	0.23	0.30	0.30	0.32	0.32	0.30	0.30	0.30
mode									
2D readout									
2D readout (full frame)									
10x10 subaps all pix	6184	847	5700	860	3346	8734	2108	6250	4156
2D readout (8x8 subapertures)									
8x8 subaps all pix	4040	624	3752	655	2266	5714	1454	4104	2764
6 x 6 pixels in box	2387	466	2257	515	1447	3387	964	2455	1701
4x4 pixels in box	1154	300	1122	348	792	1654	547	1210	875
4 x 4 big pixels	1113	259	1069	295	735	1597	494	1157	822
2 x 2 big pixels	340	127	347	153	300	516	203	369	285
1D readout (8x8 subaps)									
8 pixels in X	530	103	502	114	357	788	214	546	378
6 pixels in X in box	457	136	451	161	358	682	236	484	359
4 pixels in X in box	341	128	348	154	304	519	204	370	286
4 big pixels in X	300	87	295	102	247	463	152	317	233
2 big pixels in X	185	78	192	95	192	300	120	203	161

¹ /home/ngs/docs/xls/rctstime.xls

Appendix 5. Sky Coverage issues for an increased noise sensor.

The WFS in NAOMI contains a beamsplitter to provide illumination for 2 CCD detectors, to maximise efficiency and latency in the baseline 4x4 pixel readout mode. When we are working close to the guide star, the static off axis telescope aberrations for the guide star are compensated for by static offsets of the working control loop zero points in the WFS. Where these offsets are small, ie with the maximum spot offset less than 0.5 pixel, a quad cell geometry can be used, with a gain in signal to noise of approximately 3 over the baseline geometry.

With the quad cell geometry, there is a slight loss in signal to noise of some 5% when operating with two binned CCD's as opposed to a single 4 pixel detector. This note examines the sky coverage implications of this loss of signal to noise.

A 5% increase in noise can be compensated by a 5% increase in signal, by using a star of 0.056 magnitudes brighter. From Gemini technical note TN -PS-G0030², we can use the Bahcall -Soniera model to estimate the star density for a typical limiting case.

If we choose the brighter guide star to be $m_R = 16.25$, then we can interpolate for the change in magnitude. This gives a density of 1272 stars/degree² at $m_R=16.25$ and 1320 stars/degree² at $m_R=16.31$.

Table 8-8 Guide star densities

R mag	all-sky average.
16.25	1272
16.31	1320
16.75	1703

The probability of finding a guide star is given by the ratio of the guide star density to the area available. For a given area then the ratio of probabilities is imply the ratio of guide star densities. The relative probability of finding a 16th magnitude guide star is $1272/1320 = 0.964$.

For the 5% loss in light due to the 2CCD mode, we would thus lose 3.6 % of the available guide stars.

² Gemini Technical note TN -PS-G0030 "Longitudinally Averaged R -Band Field Star Counts Across the entire sky." Doug Simons August 1995

Appendix 6. 4x4 Baseline mode justification

Subject: Need for 4 x 4 pixelbaseline configuration for WFS
Date: Thu, 15 May 1997 17:08:01 +0100 (BST)
From: "Ronald A. Humphreys" <R.A.Humphreys@durham.ac.uk>
To: Bruce Gentles <abg@ast.cam.ac.uk>
CC: Andy Longmore <ajl@roe.ac.uk>, Mick Johnson <mrj@ast.cam.ac.uk>, Guy Rixon <gtr@ast.cam.ac.uk>, Richard Myers <R.M.Myers@durham.ac.uk>

Hi Bruce,

The purpose of this message is to briefly document the various points we made during discussions last Tuesday on the need for the 4 x 4 pixel baseline configuration. In particular the final point expresses our reluctance to expose the project to the risk of potential failure.

1. Lincoln Lab. has found that the slope of a WFS transfer curve should not vary by more than +/- 15% to provide good servo stability in closed-loop operation. With even modest spot offsets one can readily exceed this criterion in quad -cell operation. The RGO analysis did not address any effects on servo-system operation.
2. MARTINI has found that quite large and variable (with time) offset corrections were required. Even after correction with the steering mirrors the offsets remained a problem. The problems persisted over a range of subaperture sizes which included the NAOMI regime. The source(s) of these offsets is not known but it is probably associated with the WHT. The offsets calculated by RGO were under ideal conditions, i.e. all components within the NAOMI system were aligned within tolerance.
3. GEMINI has indicated that the effects of wind shake can be a serious problem.
4. Bob Fugate has experienced servo instability problems operating in a quad-cell mode whereas SWAT did not have any problems of this nature when operating in a 4 x 4 mode.
5. Considerable rigorous analysis would be required to positively prove or disprove that we do not need the 4 x 4 baseline mode. Anything less would still leave us subject to doubt.
6. We feel that the risk is that without the 4 x 4 baseline mode we may encounter conditions where the system will not close the loop properly or at all, e.g. with a faint star in moderate to strong turbulence conditions.

Cheers,

Richard and Ron.

Ron Humphreys Physics Dept, Science Labs, South Rd, Durham DH1 3LE, UK
Tel: 091 374 3712, Fax: +44 91 374 3749, Internet: R.A.Humphreys@durham.ac.uk

Appendix 7. 1D and 2D centroids

The 2D standard linear weighted calculation can be decomposed into 2 1D sums as follows.

$$centroid_x = \frac{\sum_y P_{x,y} x}{\sum_y P_{x,y}}$$

This can be re-arranged to yield

$$centroid_x = \frac{\sum_x x (\sum_y P_{x,y})}{\sum_x (\sum_y P_{x,y})}$$

$$centroid_x = \frac{\sum_x x ms_x}{\sum_x ms_x} \quad \text{where } ms_x = \sum_y P_{x,y} \text{ is the marginal sum for column } x.$$

Appendix 8. Gemini ICD 1.6.1/1.6.2 - A&G to WFS system.

